

# Zinc Tetraphenylporphyrin as High Performance Visible Light Photoinitiator of Cationic Photosensitive Resins for LED Projector 3D Printing Applications

Assi Al Mousawi,<sup>†,‡</sup> Cyril Poriel,<sup>§</sup> Frédéric Dumur,<sup>||</sup> Joumana Toufaily,<sup>‡</sup> Tayssir Hamieh,<sup>‡</sup> Jean Pierre Fouassier,<sup>†</sup> and Jacques Lalevée<sup>\*,†,§</sup>

<sup>†</sup>Institut de Science des Matériaux de Mulhouse IS2M–UMR CNRS 7361–UHA, 15, rue Jean Starcky, 68057 Mulhouse Cedex, France

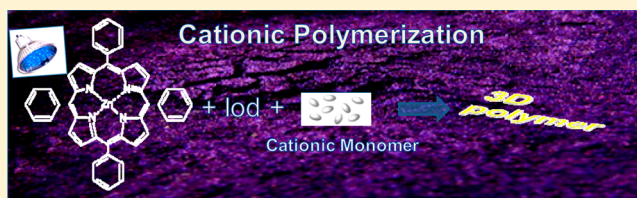
<sup>‡</sup>Laboratoire de Matériaux, Catalyse, Environnement et Méthodes analytiques (MCEMA-CHAMSI), EDST, Université Libanaise, Campus Hariri, Hadath, Beyrouth Lebanon

<sup>§</sup>Institut des Sciences Chimiques De Rennes-MaCSE Group, Université De Rennes 1-UMR CNRS 6226, Bat 10C Campus De Beaulieu, 35042 Rennes Cedex, France

<sup>||</sup>Aix Marseille Univ, CNRS, ICR UMR 7273, F-13397 Marseille, France

## S Supporting Information

**ABSTRACT:** Zinc tetraphenylporphyrin (ZnTPP) is proposed as a high performance visible light photoinitiator for both the free radical polymerization (FRP) of methacrylates (thick films) and the cationic polymerization (CP) of epoxides (thin films) upon visible light exposure using light emitting diodes (LEDs) at 405, 455, 477, and 530 nm. ZnTPP combined with an iodonium salt shows excellent polymerization initiating abilities and high final conversions were obtained. Remarkably, for the ligand alone (tetraphenylporphyrin derivative, H<sub>2</sub>TPMP) used as photoinitiator, no polymerization occurs, indicating the importance of the metal in the initiating complex for an efficient process. A full picture of the involved chemical mechanisms is given. The high performance of ZnTPP as cationic initiating system is also well shown for new cationic 3D printing resins upon exposure to LED projector at 405 nm.



## 1. INTRODUCTION

Because of many advantages (low temperature of usage, low emission of volatile organic compounds, low energetic consumption, etc.), the polymerization processes triggered or controlled by light are the subject of huge efforts.<sup>1–5</sup> More particularly, the developments of photosensitive systems that can operate at safer (longer) wavelengths than UV light are being actively researched. All of these research works are strongly supported by developments of the light emitting diodes (LEDs) that can represent very convenient irradiation devices compared to UV lamps or UV laser (e.g., mercury lamp) (see some examples in refs 1 and 6–13). Recently, 3D printers using such a LED technology (e.g., LED projector) were introduced on the market. Currently, the LED projector printing technology can be really advantageous among the 3D printing strategies; i.e., this technology projects the profile of an entire layer at one time. Therefore, the development of highly photosensitive resins is worthwhile.

In 3D printing, the use of cationic monomers associated with a ring-opening polymerization is characterized by lower shrinkage properties compared to those obtained with the radical polymerization of acrylate or methacrylate resins. In this context, the development of cationic photosensitive resins upon

visible light is highly desired. Indeed, the classical cationic initiators (iodonium, sulfonium, thianthrenium salts, etc.) absorb mainly in the UV range (<350 nm) and can hardly be used with the LED projector technology.<sup>1–6</sup>

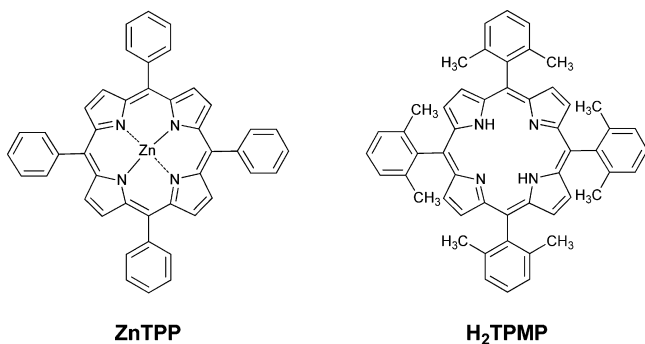
In the present paper, new photosensitive resins for the cationic polymerization of epoxides upon visible light will be proposed. The photoinitiating systems will be based on zinc tetraphenylporphyrin (ZnTPP) that is characterized by excellent light absorption properties for  $\lambda > 400$  nm. ZnTPP or its derivatives have been already characterized by a good initiating ability for free radical polymerization (FRP) processes<sup>11–13</sup> and have been employed for living radical polymerization in the presence of RAFT agent,<sup>14</sup> but never checked in cationic polymerization (CP). The comparison of the metalloporphyrin ZnTPP with the free base porphyrin H<sub>2</sub>TPMP (photochemical properties/photoinitiating ability) will be provided to show the role of the metal center (Scheme 1). The presence of eight methyl groups in H<sub>2</sub>TPMP ensures a good solubility in monomer matrixes. Therefore, this latter compound can be

**Received:** December 2, 2016

**Revised:** January 4, 2017

**Published:** January 20, 2017

Scheme 1. Investigated Chemical Compounds Used



compared to ZnTPP for which a good solubility was also observed.

Examples of the performance of the ZnTPP/iodonium salt couple as a cationic photoinitiating system in new cationic 3D printing resins upon exposure to LED projector @405 nm under air are shown. A full picture of the involved chemical mechanisms in the proposed initiating systems is also provided.

## 2. EXPERIMENTAL PART

**2.1. Chemical Compounds.** Phenyl-*N*-*tert*-butylnitrone (PBN) and ZnTPP were obtained from SigmaAldrich. Bis(4-*tert*-butylphenyl)-iodonium hexafluorophosphate (Speedcure 938 or Iod) was obtained from Lambson (U.K.). 9-(4-Hydroxyethoxyphenyl)thianthrenium hexafluorophosphate (th) was obtained from Lamberti SpA (Italy). Bisphenol A-glycidyl methacrylate (BisGMA) and triethylene glycol dimethacrylate (TEGDMA) were obtained from SigmaAldrich and used with the highest purity available. (3,4-Epoxy cyclohexane)methyl 3,4-epoxycyclohexylcarboxylate (EPOX, Uvacure 1500) was obtained from Allnex and used as benchmark monomer for cationic photopolymerization. Structures of these are shown in Scheme 2

**2.2. Synthesis of H<sub>2</sub>TPMP.** H<sub>2</sub>TPMP was synthesized from the corresponding pyrrole and 2,6-dimethylbenzaldehyde following a procedure reported<sup>15</sup> for other phenyl-ortho-substituted porphyrins. In a typical experimental procedure, pyrrole (10 mmol) and 2,6-dimethylbenzaldehyde (10 mmol) were dissolved in 1 L of degassed chloroform in a 2-L three-neck round-bottomed flask, before adding boron trifluoride diethyl etherate (3.3 mmol) via a syringe. The resulting mixture was then stirred for 1 h, at room temperature, and protected from light. After addition of *p*-chloranil (7.5 mmol), the mixture was stirred for 1 h at 60 °C. The mixture was then cooled to room temperature, triethylamine (3.3 mmol) was added, and the solution was rotary evaporated to dryness. The crude was then washed

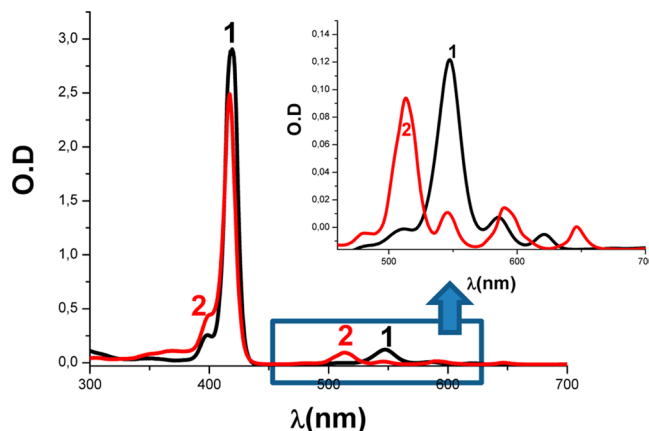


**Figure 1.** Absorption spectra of the investigated compounds in DCM: (1) ZnTPP; (2) H<sub>2</sub>TPMP.

with methanol, filtered and washed with petroleum ether to afford H<sub>2</sub>TPMP with 20% yield. The spectroscopic analyses and purity of H<sub>2</sub>TPMP were in accordance with previous works.<sup>16</sup>

**2.3. Irradiation Sources.** The following light emitting diodes (LEDs) were used as irradiation sources: (i) LED@375 nm - incident light intensity at the sample surface,  $I_0 \approx 40 \text{ mW cm}^{-2}$ ; (ii) LED@405 nm ( $I_0 \approx 110 \text{ mW cm}^{-2}$ ); (iii) LED projector @405 nm for 3D printing ( $I \approx 100\text{--}130 \text{ mW cm}^{-2}$ ); (iv) LED@455 nm ( $I_0 \approx 80 \text{ mW cm}^{-2}$ ); (v) LED@477 nm ( $I_0 \approx 300 \text{ mW cm}^{-2}$ ); (vi) LED@530 nm ( $I_0 \approx 30 \text{ mW cm}^{-2}$ ).

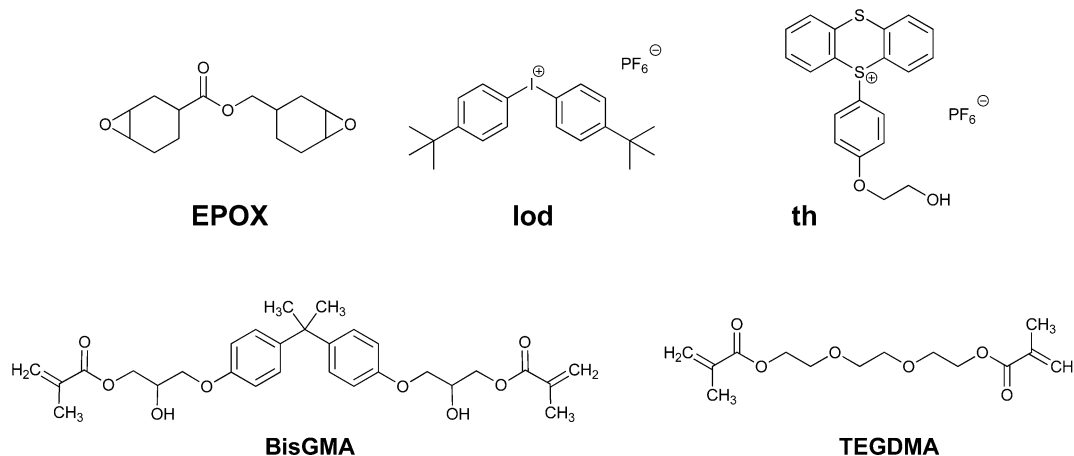
**2.4. Cationic Photopolymerization (CP) and Free Radical Photopolymerization (FRP).** The two-component photoinitiating systems (PISs) are mainly based on H<sub>2</sub>TPMP/iodonium salt or ZnTPP/iodonium salt (0.5%/1% w/w) for both CP and FRP. The weight percent of the photoinitiating system is calculated from the monomer content. The photosensitive thin formulations ( $\sim 25 \mu\text{m}$  of thickness) were deposited on BaF<sub>2</sub> pellets under air for the CP of EPOX. The 1.4 mm thick samples of BisGMA/TEGDMA were also polymerized under air.

The evolution of the epoxy group content and the double bond content of methacrylate functions were continuously followed by real time FTIR spectroscopy (JASCO FTIR 4100) at about 790 and 1630  $\text{cm}^{-1}$ , respectively. The evolution of the methacrylate characteristic peak for the thick samples (1.4 mm) was followed in the near-infrared range at  $\sim 6160 \text{ cm}^{-1}$ .

The procedure used to monitor the photopolymerization profile has been described in details in.<sup>6,17,18</sup>

**2.5. Free Energy Calculations for Electron Transfer.** The free energy change  $\Delta G_{\text{et}}$  for an electron transfer reaction was calculated

Scheme 2. Other Used Chemical Compounds



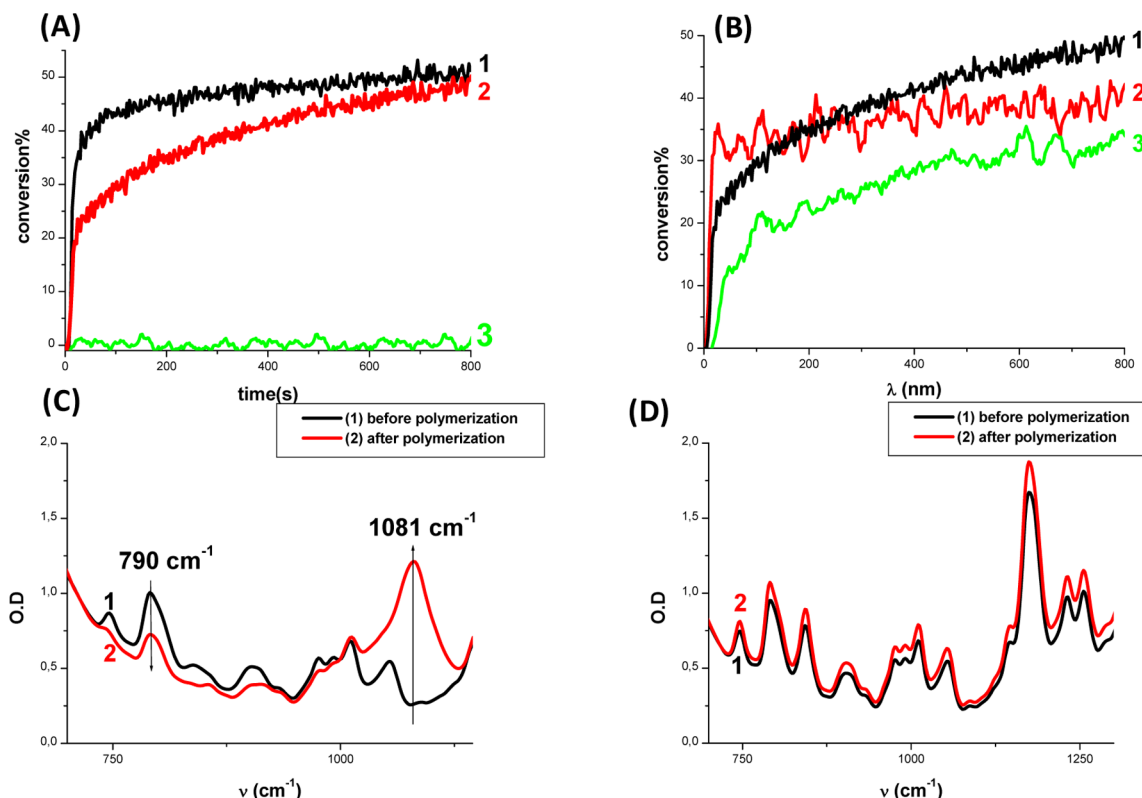


**Figure 2.** (A) Polymerization profiles (epoxy function conversion vs irradiation time) for EPOX under air (thickness = 25 μm) upon exposure to LED@405 nm in the presence of the two-component photoinitiating systems: (1) ZnTPP/Iod (0.5%/1% w/w); (2) ZnTPP/Iod (0.3%/1% w/w); (3) H<sub>2</sub>TPMP/Iod (0.5%/1% w/w). The irradiation starts for  $t = 10$  s. (B) Polymerization profiles (epoxy function conversion vs irradiation time) for EPOX under air (thickness = 25 μm) in the presence of the two-component photoinitiating system ZnTPP/Iod (0.3%/1% w/w) upon exposure to various LEDs: (1) LED@405 nm; (2) LED@455 nm; (3) LED@530 nm. The irradiation starts for  $t = 10$  s. (C) IR spectra recorded before and after polymerization for ZnTPP/Iod (0.5%/1% w/w) upon exposure to LED@405 nm. (D) IR spectra recorded before and after polymerization for H<sub>2</sub>TPMP/Iod (0.5%/1% w/w) upon exposure to LED@405 nm.

**Table 1.** Final Epoxy Function Conversion (FC) for the EPOX and Methacrylate (BisGMA/TEDGMA) Functions after 800 and 100 s of Irradiation, Respectively, and the Role of Different LEDs

	% epoxy function conversion (FC) (at $t = 800$ s)		% methacrylate function conversion (FC) (at $t = 100$ s)
	ZnTPP/Iod (thickness = 25 μm) under air	H <sub>2</sub> TPMP/Iod (thickness = 25 μm) under air	ZnTPP/Iod (thickness = 1.4 mm) under air
LED@405 nm	53% (0.5%/1% w/w); 47% (0.3%/1% w/w)	(0.5%/1% w/w) <sup>a</sup> n.p.	12% (0.3%/1% w/w)
LED@455 nm	39% (0.3%/1% w/w)		28% (0.3%/1% w/w)
LED@477 nm			70% (at $t = 80$ s) (0.3%/1% w/w)
LED@530 nm	33% (0.3%/1% w/w)		50% (0.3%/1% w/w)

<sup>a</sup>n.p.: no polymerization.

from the classical Rehm–Weller equation eq 1<sup>19</sup> where  $E_{ox}$ ,  $E_{red}$ ,  $E_S$ , and  $C$  are the oxidation potential of the electron donor, the reduction potential of the electron acceptor, the excited state energy and the Coulombic term for the initially formed ion pair, respectively.  $C$  is neglected as usually done in polar solvents.

$$\Delta G_{et} = E_{ox} - E_{red} - E_S + C \quad (1)$$

**2.6. ESR Spin-Trapping (ESR-ST) Experiments.** The ESR-ST experiments were carried out using an X-Band spectrometer (Mini-Scope MS400-Magnetech). LED@477 nm was used as irradiation source for triggering the production of radicals at room temperature (RT) under N<sub>2</sub> in *tert*-butylbenzene and trapped by phenyl-*N*-*tert*-butylnitron (PBN) according to a procedure described elsewhere in detail.<sup>17,18</sup> The ESR spectra simulations were carried out with the PEST WINSIM program.

**2.7. Absorption Experiments.** The absorbance properties of the compounds as well as the steady state photolysis experiments were studied using a JASCO V730 spectrometer.

**2.8. Fluorescence Experiments.** The fluorescence properties of the compounds were studied using a JASCO FP-6200 spectrometer.

**2.9. 3D Printing Experiments.** For 3D printing experiments, a LED@405 nm projector (Thorlabs) was used. Rather similar intensity on the surface of the sample and similar emission spectrum for the LED used in 3D printing and the LED in kinetic experiments were used for sake of comparison. The photosensitive cationic resin was polymerized under air and the generated shapes analyzed by a numerical optical microscope (DSX-HRSU from OLYMPUS corporation) or by profilometry.

**2.10. Laser Flash Photolysis.** Nanosecond laser flash photolysis (LFP) experiments were carried out using a Luzchem LFP 212 spectrometer. For the excitation, a Q-switched nanosecond Nd/YAG laser

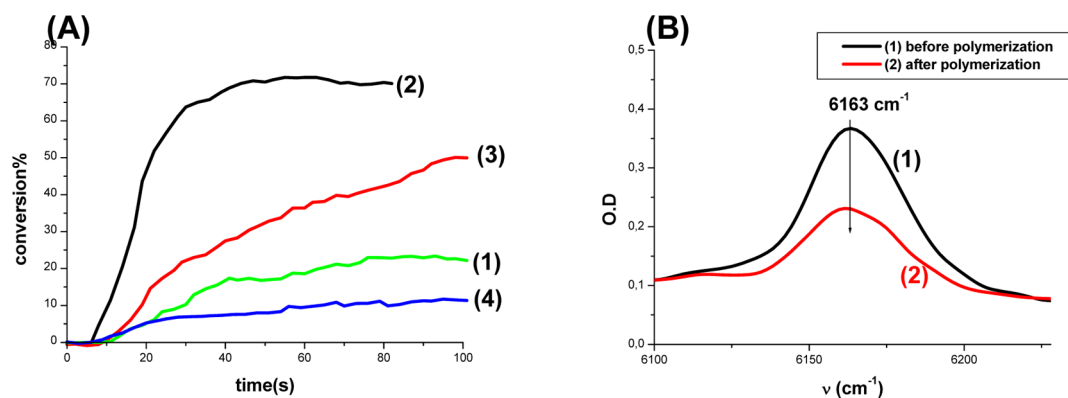


**Figure 3.** Polymerization profiles (methacrylate function conversion vs irradiation time) for BisGMA/TEGDMA under air (thickness = 1.4 mm) in the presence of the two-component photoinitiating system ZnTPP/Iod (0.3%/1% w/w) upon exposure to various irradiation sources: (1) LED@455 nm; (2) LED@477 nm; (3) LED@530 nm; (4) LED@405 nm. (B) IR spectra recorded before and after polymerization for ZnTPP/Iod (0.3%/1% w/w) upon exposure to LED@530 nm. The irradiation starts for  $t = 10$  s.

( $\lambda_{\text{exc}} = 355$  nm,  $\sim 6$  ns pulses; energy reduced down to 10 mJ) from Continuum (Minilite) was used.<sup>17,18</sup>

### 3. RESULTS AND DISCUSSION

**3.1. Light Absorption Properties of the Investigated Compounds.** The absorption spectra of the new proposed photoinitiators/photosensitizers (ZnTPP and H<sub>2</sub>TPMP) in dichloromethane (DCM) are reported in Figure 1. These compounds are characterized by (i) a main band (called Soret band or B Band), which possesses extremely high extinction coefficients in the blue region and (ii) three (for ZnTPP) or four (for H<sub>2</sub>TPMP) additional bands (called Q bands) at higher wavelengths, which possess lower extinction coefficients (e.g., ZnTPP  $\sim 400\,000\text{ M}^{-1}\cdot\text{cm}^{-1}$  at  $\lambda_{\text{max}} = 420$  nm (B band) and  $\sim 20\,000\text{ M}^{-1}\cdot\text{cm}^{-1}$  at  $\lambda = 552$  nm (Q-band)).<sup>20,21</sup> Remarkably, their absorptions are intense in the 300–550 nm spectral range ensuring fairly good overlap with the emission spectra of the near UV or visible LEDs used in this work (e.g., at 375, 405, 455, 477, and 530 nm). The presence of zinc within the porphyrin ring plays an important role on the light absorption properties, leading in the present case (despite the porphyrin rings are slightly differently substituted) to a bathochromic shift of 30 nm of the lowest energy transition.

**3.2. Cationic Photopolymerization (CP) of Epoxides.** The CP of 25  $\mu\text{m}$  thick epoxide films (e.g., EPOX) under air exhibits a very high efficiency in term of final epoxy function conversion (FC), e.g., FC = 53% with ZnTPP (Figure 2A, curve 1; Table 1), using two-component photoinitiating systems based on ZnTPP/Iod combinations (0.5%/1% w/w) upon irradiation with the LED@405 nm. The same holds true at lower concentrations of ZnTPP (e.g., FC = 47% with ZnTPP (0.3% w/w); Figure 2A, curve 2, Table 1). In the same context, good polymerization profiles are also obtained when using various LEDs (e.g., FC = 39% with LED @455 nm; Figure 2B, curve 2, Table 1). In addition, a new peak ascribed to the formation of the polyether network during the photopolymerization arises at  $\sim 1080\text{ cm}^{-1}$  in the FTIR spectra (Figure 2C). In these irradiation conditions, Iod alone does not work showing the sensitizer behavior of ZnTPP. For comparison, ZnTPP/th (0.5%/1% w/w) was tested and no polymerization was observed using LED@405 nm under air. Therefore, ZnTPP can be considered as a good photoinitiator in combination with an iodonium salt but not with thianthrenium salt (see the chemical mechanisms in part 3.5). Remarkably, no

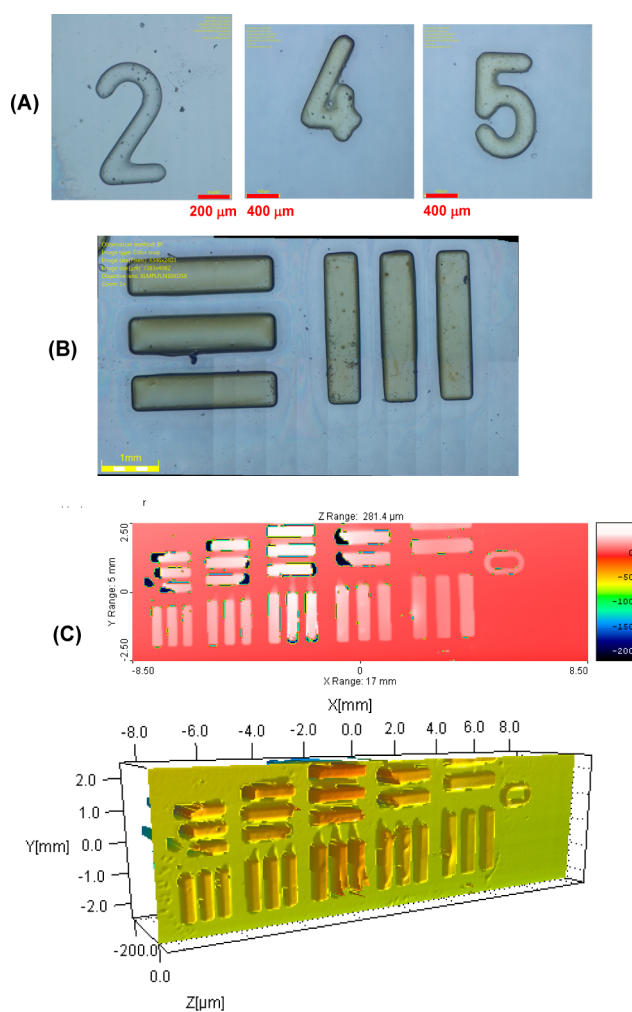


**Figure 4.** 3D-Photopolymerization experiments using projector LED@405 nm: different numbers (2, 4, 5) in part A or patterns in part B written can be easily observed by a numerical optical microscope; in part C, the patterns are characterized in 3D by profilometry.

polymerization was observed when using the H<sub>2</sub>TPMP/Iod system (0.5%/1% w/w) with LED@405 nm (Figure 2A, curve 3, and also Figure 2D) showing the huge effect of the Zn metal center on the photochemical properties and the associated initiating ability.



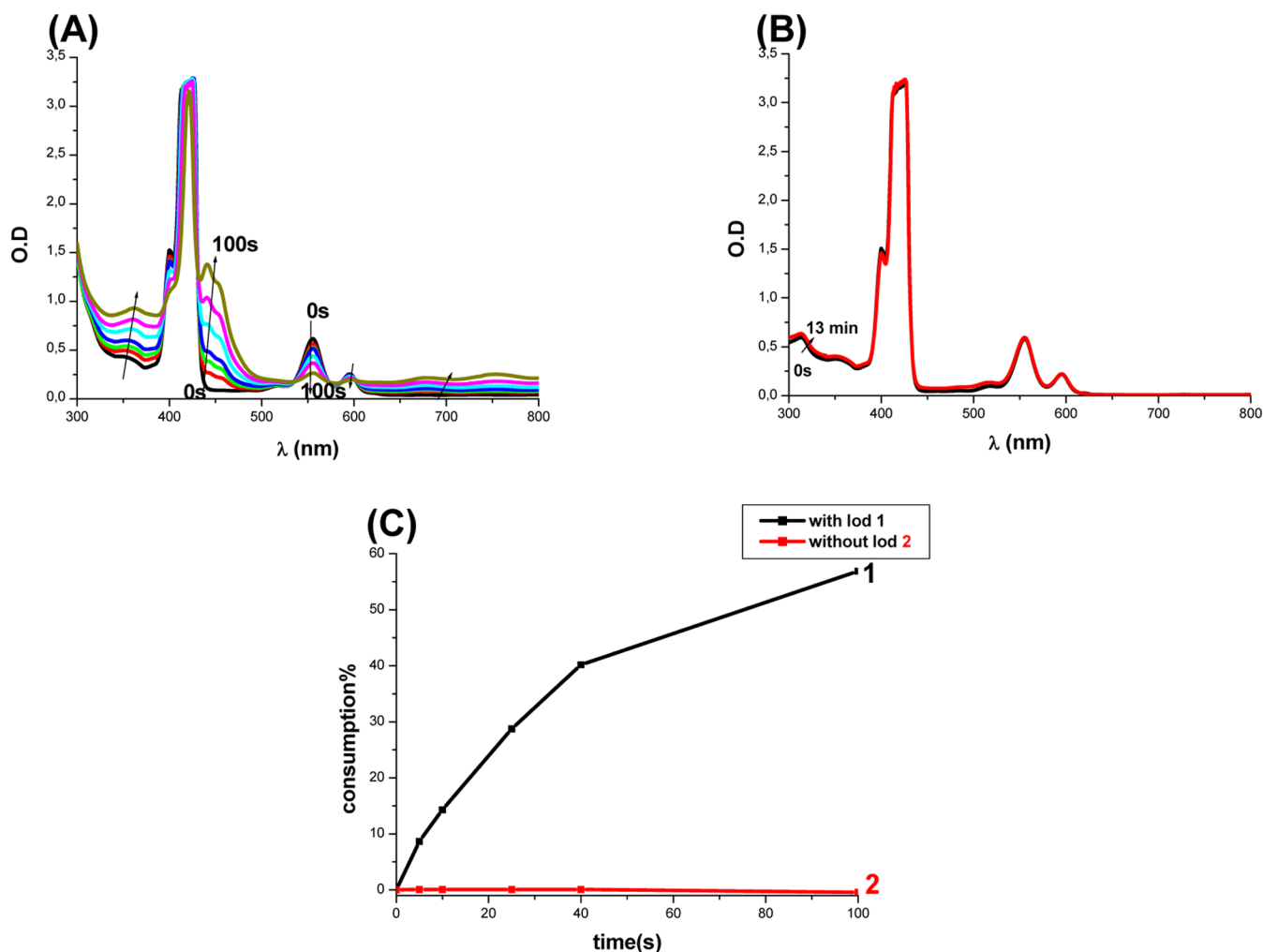


**Figure 5.** (A) ZnTPP/Iod photolysis upon exposure with LED@375 nm and (B) photolysis of ZnTPP in absence of Iod. (C) Consumption (%) of ZnTPP with (1) and without (2) Iod salt vs time of irradiation with a LED@375 nm.

**3.3. Free Radical Photopolymerization of BisGMA/TEGDMA.** The FRP of BisGMA/TEGDMA in thick films (1.4 mm) under air and in the presence of the ZnTPP/Iod (0.3%/1% w/w) couple is very efficient using different LEDs (e.g., LED@477 nm and LED@530 nm) (Figure 3). Clearly, ZnTPP/Iod PIS has the ability to overcome the oxygen inhibition usually observed in FRP. This excellent ZnTPP behavior is in full agreement with oxygen tolerance techniques found in.<sup>22</sup> Typical methacrylate function conversion–time profiles are given in Figures 3A and the FCs are summarized in Table 1. In these irradiation conditions, Iod alone does not work. H<sub>2</sub>TPMP/Iod (0.3%/1% w/w) couple is not able to initiate the FRP of methacrylates. The LED@477 nm irradiation leads to the highest rate of polymerization ( $R_p$ ) and final conversion (Figure 3A curves 1, 2, and 3; see also in Table 1). This can be ascribed to the much higher intensity of the LED@477 nm (300 mW/cm<sup>2</sup> - see the experimental part). Note that the color of the obtained thick polymer remains dark colored suggesting rather poor bleaching properties during the course of the polymerization.

**3.4. Surface Patterning or 3D Printing Using the ZnTPP-Based System upon LED Projector.** The ZnTPP/Iod (0.3%/1% w/w) photoinitiating system being very reactive for the cationic polymerization under air (EPOX—see above), some 3D printing experiments upon a LED projector @405 nm

were carried out (Figure 4). Indeed, the high photosensitivity of this resin allows an efficient polymerization process in the irradiated area. The cationic process upon LED @405nm projector can be useful to reduce the shrinkage usually observed for radical polymerization in 3D printing. The 3D written patterns are well characterized with optical microscopy (Figure 4, parts A and B) or profilometry (Figure 4C) experiments. The objects are obtained by projection of an entire layer at one time for each layer. The light intensity is quite low (100–130 mW/cm<sup>2</sup>) showing the good performance of the proposed system.

**3.5. Chemical Mechanisms. 3.5.1. Steady State Photolysis.** The steady state photolysis of ZnTPP/Iod in acetonitrile upon irradiation with a LED@375 nm is very fast, compared to the very high photostability of ZnTPP alone where no photolysis occurs (e.g., ZnTPP/Iod in Figure 5A vs ZnTPP alone in Figure 5B). A new photoproduct (characterized by significant new absorptions for 430 nm > λ > 510 nm and for λ > 600 nm) is formed in any case which, accordingly, is due to the ZnTPP/Iod interaction.

**3.5.2. Fluorescence Quenching, Cyclic Voltammetry, Laser Flash Photolysis, and ESR Experiments.** Fluorescence and fluorescence quenching experiments in acetonitrile for ZnTPP/Iod are shown in Figure 6. First, the crossing point of the absorption and fluorescence spectra allows the determination of

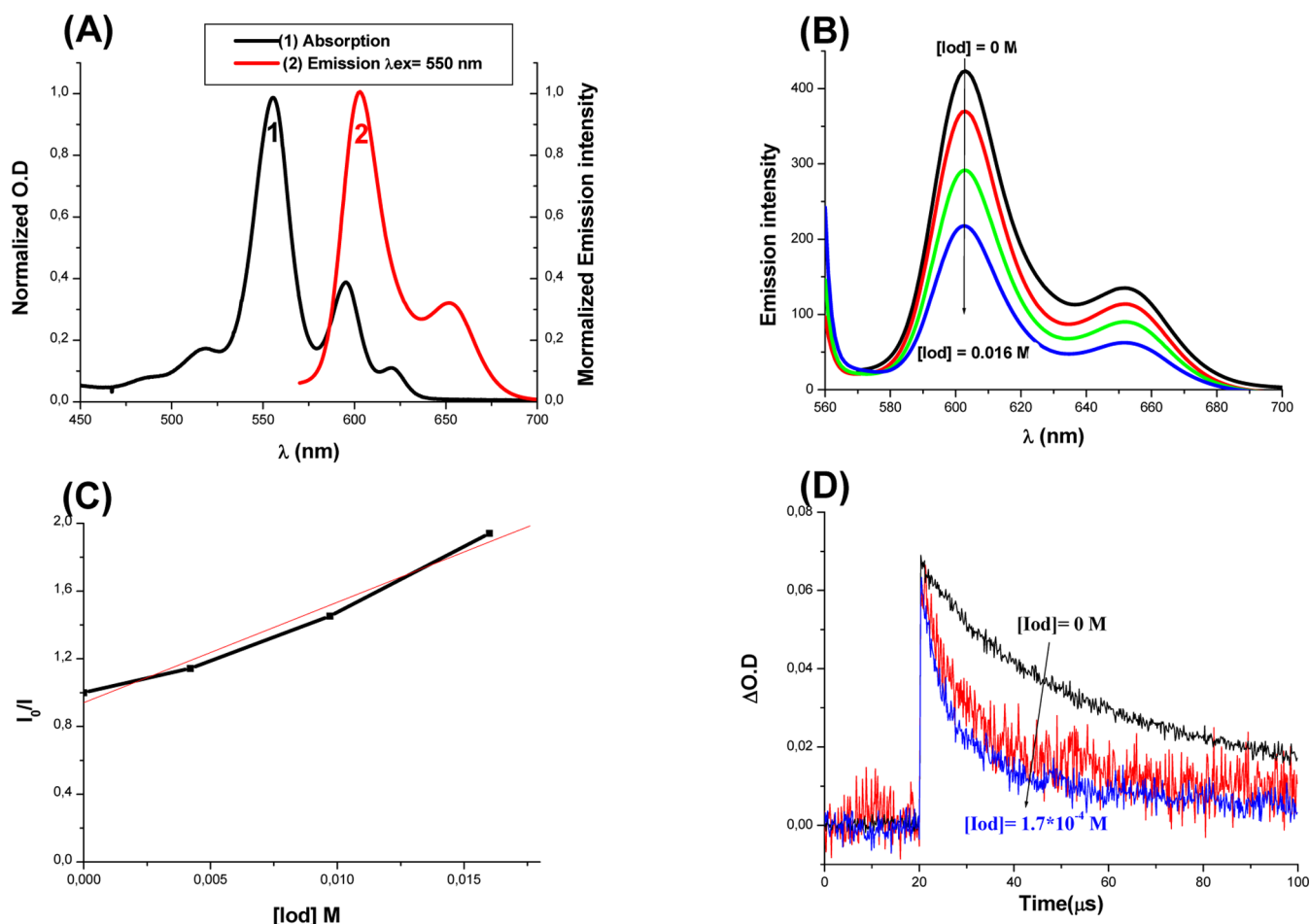


**Figure 6.** (A) Singlet state energy determination in acetonitrile; (B) fluorescence quenching of  $^1\text{ZnTPP}/\text{Iod}$ ; (C) Stern–Volmer treatment for the  $^1\text{ZnTPP}/\text{Iod}$  fluorescence quenching; (D) kinetics observed at 470 nm in laser flash photolysis for the laser excitation of a ZnTPP solution in acetonitrile (laser excitation for  $t = 20 \mu\text{s}$ ). The lifetime of  $^3\text{ZnTPP}$  decreases in the presence of Iod.

**Table 2. Parameters Characterizing the Chemical Mechanisms Associated with  $^1,^3\text{ZnTPP}/\text{Iod}$  and  $^1,^3\text{ZnTPP}/\text{th}$  (in Acetonitrile) and  $^1\text{H}_2\text{TPMP}/\text{Iod}$  (in DCM)<sup>a</sup>**

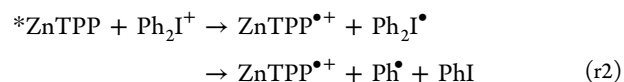
	$E_{\text{ox}}$ [V]	$E_{\text{S1}}$ [eV]	$\Delta G_{\text{et(S1)}}$ [eV]	$K_{\text{sv}}$ ( $\text{M}^{-1}$ )	$\Phi_{\text{et(S1)}}$	$E_{\text{T1}}$ [eV]	$\Delta G_{\text{et(T1)}}$ [eV]
ZnTPP/Iod	0.78	2.11	−1.13	59.3	0.6	1.59 <sup>c</sup>	−0.61
ZnTPP/th	0.78	2.11	−0.12	n.q. <sup>b</sup>	<0.1	1.59 <sup>c</sup>	+0.39
$\text{H}_2\text{TPMP}/\text{Iod}$	1.05	1.99	−0.65				

<sup>a</sup>Reduction potentials of −0.2 V and −1.2 V were used for Iod and th, respectively,<sup>1</sup> in eq 1 for the calculations of  $\Delta G_{\text{et}}$  with the singlet state of ZnTPP ( $\Delta G_{\text{et(S1)}}$ ) or the triplet state of ZnTPP ( $\Delta G_{\text{et(T1)}}$ ). <sup>b</sup>n.q.: no fluorescence quenching observed. <sup>c</sup>From ref 26.

the first excited singlet state energy ( $E_{\text{S1}}$ ) (Table 2). Favorable  $^1\text{ZnTPP}/\text{Iod}$  fluorescence quenching process was shown with (i) high value of the Stern–Volmer coefficients ( $K_{\text{sv}}$ ; Table 2), (ii) high electron transfer quantum yield ( $\Phi_{\text{et}}$ ) (calculated according to eq 2, Table 2), and (iii) the highly favorable free energy changes ( $\Delta G_{\text{et}}$ ) for the expected electron transfer reaction (reactions r1 and r2; e.g., for ZnTPP/Iod,  $\Delta G_{\text{et}} = -1.13 \text{ eV}$ ; see Table 2; the potential of the first oxidation peak of ZnTPP was determined by cyclic voltammetry at 0.75 V in full agreement with the literature data from refs 23 and 24).

Taking into account the lifetime for the first excited state of ZnTPP (1.8 ns),<sup>25</sup> the rate constant for the electron transfer  $^1\text{ZnTPP}/\text{Iod}$  is found very high and diffusion controlled ( $k = 3 \times 10^{10} \text{ M}^{-1} \text{ s}^{-1}$ ).

$$\Phi_{\text{et}} = K_{\text{sv}}[\text{Iod}]/(1 + K_{\text{sv}}[\text{Iod}]) \quad (2)$$



A triplet state pathway can not be ruled out i.e. the free energy change ( $\Delta G_{\text{et(T1)}}$ ) for the electron transfer reaction  $^3\text{ZnTPP}/\text{Iod}$  is also favorable (Table 2). Indeed, laser flash photolysis experiments for ZnTPP solution were performed in acetonitrile under  $\text{N}_2$  and the lifetime of the triplet state of ZnTPP was calculated to be  $\sim 65 \mu\text{s}$  (Figure 6D). In the presence of Iod, a clear quenching of  $^3\text{ZnTPP}$  is observed (Figure 6D); the  $^3\text{ZnTPP}/\text{Iod}$  electron transfer rate constant is  $\sim 4.310^8 \text{ M}^{-1} \text{ s}^{-1}$  using a Stern–Volmer plot,<sup>1</sup> but this rate constant is lower than that for the  $^1\text{ZnTPP}/\text{Iod}$  electron transfer (see above). This is in full agreement with the respective  $\Delta G$

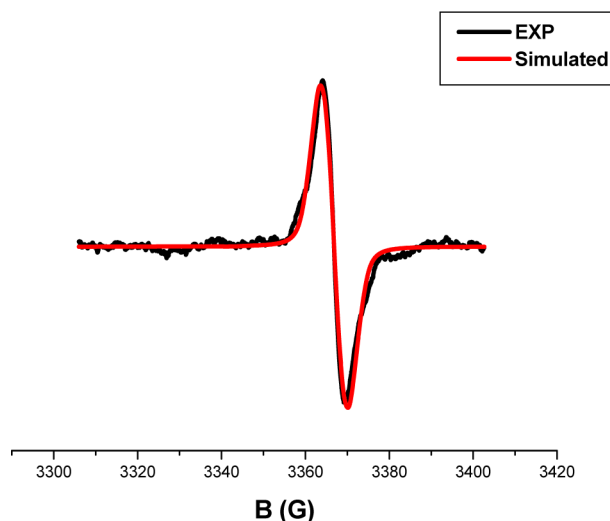


**Figure 7.** ESR spectrum obtained upon irradiation (LED@477 nm) of a ZnTPP/Iod solution. Solvent = *tert*-butyl benzene.

values from  $^1\text{ZnTPP}$  and  $^3\text{ZnTPP}$ :  $\Delta G_{\text{et}(T_1)} = -0.61$  eV is less favorable than  $\Delta G_{\text{et}(S_1)} = -1.13$  eV; see Table 2.

The favorable quenching process of  $^*\text{ZnTPP}$  by Iod results from reactions r1 and r2. This is also confirmed by ESR results. Indeed, the phenyl radicals ( $\text{Ph}^\bullet$ ) were easily detected in a ZnTPP/Iod irradiated solution as PBN/ $\text{Ph}^\bullet$  radical adducts, the hyperfine coupling constants (hfcs) being  $a_N = 14.05$  G and  $a_H = 2.1$  G (typical for the PBN/ $\text{Ph}^\bullet$  radical adducts<sup>17,18</sup>).

On the other side, the radical cation ( $\text{ZnTPP}^{\bullet+}$ ) was easily detected in the irradiated ZnTPP/Iod system (Figure 7) where no spin trap agent (PBN) was used to avoid detecting any additional phenyl radical. The ESR spectrum of  $\text{ZnTPP}^{\bullet+}$  consists of broad line pattern at  $g = 2.0027$  in full accordance with<sup>27</sup> (however, it was impossible to resolve the hyperfine structure at room temperature due to the modulation of the ESR spectrometer (1 G)).

$\text{Ph}^\bullet$  and  $\text{ZnTPP}^{\bullet+}$  can be considered as the initiating species for the radical polymerization and the cationic polymerization, respectively.

**3.5.3. Structure/Reactivity/Efficiency Relationship.** Although both ZnTPP and  $\text{H}_2\text{TPMP}$  have very high and rather similar extinction coefficients at 405 nm ( $\epsilon \sim 60\,000\text{ M}^{-1}\text{ cm}^{-1}$  for both), only the ZnTPP/Iod system was able to initiate the cationic polymerization (Figure 2A curves 1 vs curve 3). This can be ascribed to the more favorable free energy of the electron transfer in ZnTPP/Iod over both ZnTPP/th and  $\text{H}_2\text{TPMP}$ /Iod ( $\Delta G_{\text{et}} = -1.12$  eV compared to  $\Delta G_{\text{et}} = -0.12$  eV and  $\Delta G_{\text{et}} = -0.65$  eV respectively; Table 2). ZnTPP is crucial and is responsible for the high performance of this system. Remarkably, other metalloporphyrin derivatives such as Fe(III) Cl TDMPP and Mn(III)Cl TDMPP (Scheme S1) do not exhibit any initiating ability for CP (Figure S1). Therefore, ZnTPP can be considered as a quite unique metalloporphyrin derivative for CP.

## 4. CONCLUSION

In the present paper, ZnTPP is proposed as a high performance visible light photoinitiator for the cationic polymerization of epoxides. The comparison of the metalloporphyrin ZnTPP with the free base porphyrin  $\text{H}_2\text{TPMP}$  (photochemical properties/photoinitiating ability) clearly shows the role of the metal (Zn) to obtain an efficient initiation process both in FRP

and in CP. The high performance of ZnTPP as cationic initiating system is also shown for new cationic 3D printing resins upon exposure to LED projector. The development of other high performance photosensitive resins for 3D printing (for LED projector, LCD screen, etc.) is under way.

## ■ ASSOCIATED CONTENT

### § Supporting Information

The Supporting Information is available free of charge on the ACS Publications website at DOI: 10.1021/acs.macromol.6b02596.

Scheme S1, the chemical structures of other metalloporphyrins used, and Figure S1, polymerization profiles for EPOX under air (PDF)

## ■ AUTHOR INFORMATION

### Corresponding Author

\*(J.L.) E-mail: jacques.lalevee@uha.fr.

### ORCID

Cyril Poriel: 0000-0002-6036-1778

Jacques Lalevée: 0000-0001-9297-0335

### Notes

The authors declare no competing financial interest.

## ■ ACKNOWLEDGMENTS

The Lebanese group would like to thank “The Association of Specialization and Scientific Guidance” (Beirut, Lebanon) for funding and supporting this work. All of the authors thank the company “Photon&Polymers” (Dr. K. Zahouily and T. Kavalli) (Lutterbach, France) for help in the profilometry experiments. All the authors thank the Agence Nationale de la recherche (ANR) for the grant “FastPrinting”.

## ■ REFERENCES

- (1) Fouassier, J.-P.; Lalevée, J. *Photoinitiators for Polymer Synthesis, Scope, Reactivity, and Efficiency*; Wiley-VCH Verlag GmbH & Co.KGaA: Weinheim, Germany, 2012.
- (2) Fouassier, J. P. *Photoinitiator, Photopolymerization and Photocuring: Fundamentals and Applications*; Gardner Publications: New York, 1995.
- (3) Dietliker, K. A. *Compilation of Photoinitiators Commercially Available for UV Today*; Sita Technology Ltd.: London, 2002.
- (4) Davidson, S. *Exploring the Science, Technology and Application of UV and EB Curing*; Sita Technology Ltd.: London, 1999.
- (5) Crivello, J. V.; Dietliker, K.; Bradley, G. *Photoinitiators for Free Radical Cationic & Anionic Photopolymerisation*; John Wiley & Sons: Chichester, U.K., 1999.
- (6) Dietlin, C.; Schweizer, S.; Xiao, P.; Zhang, J.; Morlet-Savary, F.; Graff, B.; Fouassier, J.-P.; Lalevée, J. Photopolymerization upon LEDs: New Photoinitiating Systems and Strategies. *Polym. Chem.* **2015**, *6* (21), 3895–3912.
- (7) Treat, N. J.; Fors, B. P.; Kramer, J. W.; Christianson, M.; Chiu, C.-Y.; Read de Alaniz, J.; Hawker, C. J. Controlled Radical Polymerization of Acrylates Regulated by Visible Light. *ACS Macro Lett.* **2014**, *3* (6), 580–584.
- (8) Pan, X.; Lamson, M.; Yan, J.; Matyjaszewski, K. Photoinduced Metal-Free Atom Transfer Radical Polymerization of Acrylonitrile. *ACS Macro Lett.* **2015**, *4* (2), 192–196.
- (9) Boyer, C.; Corrigan, N. A.; Jung, K.; Nguyen, D.; Nguyen, T.-K.; Adnan, N. N. M.; Oliver, S.; Shanmugam, S.; Yeow, J. Copper-Mediated Living Radical Polymerization (Atom Transfer Radical Polymerization and Copper(0) Mediated Polymerization): From Fundamentals to Bioapplications. *Chem. Rev.* **2016**, *116* (4), 1803–1949.

- (10) Tasdelen, M. A.; Yilmaz, G.; Iskin, B.; Yagci, Y. Photoinduced Free Radical Promoted Copper(I)-Catalyzed Click Chemistry for Macromolecular Syntheses. *Macromolecules* **2012**, *45* (1), 56–61.
- (11) Corrigan, N.; Xu, J.; Boyer, C. A Photoinitiation System for Conventional and Controlled Radical Polymerization at Visible and NIR Wavelengths. *Macromolecules* **2016**, *49* (9), 3274–3285.
- (12) Yeow, J.; Shanmugam, S.; Corrigan, N.; Kuchel, R. P.; Xu, J.; Boyer, C. A Polymerization-Induced Self-Assembly Approach to Nanoparticles Loaded with Singlet Oxygen Generators. *Macromolecules* **2016**, *49* (19), 7277–7285.
- (13) Kim, D.; Stansbury, J. W. A Photo-Oxidizable Kinetic Pathway of Three-Component Photoinitiator Systems Containing Porphyrin Dye (ZnTPP), an Electron Donor and Diphenyl Iodonium Salt. *J. Polym. Sci., Part A: Polym. Chem.* **2009**, *47* (12), 3131–3141.
- (14) Shanmugam, S.; Xu, J.; Boyer, C. Exploiting Metalloporphyrins for Selective Living Radical Polymerization Tunable over Visible Wavelengths. *J. Am. Chem. Soc.* **2015**, *137* (28), 9174–9185.
- (15) Lindsey, J. S.; Wagner, R. W. Investigation of the Synthesis of Ortho-Substituted Tetraphenylporphyrins. *J. Org. Chem.* **1989**, *54* (4), 828–836.
- (16) Woon, T. C.; Shirazi, A.; Bruce, T. C. Proton NMR Investigation of iron(III) 5,10,15,20-tetrakis(2,6-Disubstituted Phenyl)porphyrins. Isolation and Characterization of Hydroxy-Ligated (5,10,15,20-tetrakis(2,6-difluorophenyl)porphyrinato)iron(III). *Inorg. Chem.* **1986**, *25* (21), 3845–3846.
- (17) Lalevée, J.; Blanchard, N.; Tehfe, M.-A.; Morlet-Savary, F.; Fouassier, J. P. Green Bulb Light Source Induced Epoxy Cationic Polymerization under Air Using Tris(2,2'-bipyridine)ruthenium(II) and Silyl Radicals. *Macromolecules* **2010**, *43* (24), 10191–10195.
- (18) Lalevée, J.; Blanchard, N.; Tehfe, M.-A.; Peter, M.; Morlet-Savary, F.; Gimes, D.; Fouassier, J. P. Efficient Dual Radical/Cationic Photoinitiator under Visible Light: A New Concept. *Polym. Chem.* **2011**, *2* (9), 1986–1991.
- (19) Rehm, D.; Weller, A. Kinetics of Fluorescence Quenching by Electron and H-Atom Transfer. *Isr. J. Chem.* **1970**, *8*, 259–271.
- (20) Morandeira, A.; Vauthey, E.; Schuwey, A.; Gossauer, A. Ultrafast Excited State Dynamics of Tri- and Hexaporphyrin Arrays. *J. Phys. Chem. A* **2004**, *108* (27), 5741–5751.
- (21) Li, Y. Solvent Effects on Photophysical Properties of Copper and Zinc Porphyrins. *Chin. Sci. Bull.* **2008**, *53* (23), 3615.
- (22) Shanmugam, S.; Xu, J.; Boyer, C. Photoinduced Electron Transfer–Reversible Addition–Fragmentation Chain Transfer (PET-RAFT) Polymerization of Vinyl Acetate and N-Vinylpyrrolidinone: Kinetic and Oxygen Tolerance Study. *Macromolecules* **2014**, *47*, 4930–4942.
- (23) Paul-Roth, C.; Rault-Berthelot, J.; Simonneaux, G.; Poriol, C.; Abdalilah, M.; Letessier, J. Electroactive Films of Poly-(tetraphenylporphyrins) with Reduced Bandgap. *J. Electroanal. Chem.* **2006**, *597* (1), 19–27.
- (24) Seely, G. R. The Energetics of Electron-Transfer Reactions of Chlorophyll and Other Compounds. *Photochem. Photobiol.* **1978**, *27* (5), 639–654.
- (25) Banerji, N.; Bhosale, S. V.; Petkova, I.; Langford, S. J.; Vauthey, E. Ultrafast Excited-State Dynamics of Strongly Coupled Porphyrin/Core-Substituted-Naphthalenediimide Dyads. *Phys. Chem. Chem. Phys.* **2011**, *13* (3), 1019–1029.
- (26) Chrysoschoos, J.; Beyene, K. Oxidative Fluorescence Quenching of Zinc Tetraphenylporphyrin (ZnTPP) by Trivalent Lanthanide Ions in Several Solvents: Role of Lanthanide-Induced Singlet–triplet Crossing. *J. Lumin.* **1999**, *81* (3), 209–218.
- (27) Takeda, Y.; Takahara, S.; Kobayashi, Y.; Misawa, H.; Sakuragi, H.; Tokumaru, K. Isoporphyrins. Near-Infrared Dyes with Noticeable Photochemical and Redox Properties. *Chem. Lett.* **1990**, *19* (11), 2103–2106.